Cement & Concrete Composites 37 (2013) 205–214

Contents lists available at SciVerse ScienceDirect

Cement & Concrete Composites

journal homepage: www.elsevier.com/locate/cemconcomp

Impact response of lightweight mortars containing expanded perlite

Derek Kramar, Vivek Bindiganavile *

Department of Civil and Environmental Engineering, University of Alberta, Edmonton, Canada T6G 2W2

ARTICLE INFO

Article history:
Received 28 September 2009
Received in revised form 9 October 2012
Accepted 10 October 2012
Available online 23 October 2012

Keywords:
Fibre reinforcement
Drop-weight impact
Relative density
Expanded perlite
Fracture toughness
Stress-rate sensitivity

ABSTRACT

This paper describes the mechanical response of lightweight mortars subjected to impact loading in flexure. Expanded perlite aggregate with a bulk density of 64 kg/m^3 was used at between 0 and 8 times by volume of Portland cement to yield a range of mortars with density between 1000 and 2000 kg/m^3. Some specimens were reinforced with a polypropylene microfibre at 0.1% volume fraction and the dynamic fracture toughness was evaluated by means of an instrumented drop-weight impact system. Companion tests were carried out in compression under quasi-static loading to standardise the mixes. The compressive strength and elastic modulus scale as the cube of the relative density, defined as the ratio of the density of the mortar to that of Portland cement paste. Whereas the flexural strength and fracture toughness were both linearly proportional to the relative density of the mortar under quasi-static loading, there was an increase in their sensitivity to relative density at higher loading rates. Contrary to what is seen in regular concrete, fibre reinforcement led to an increase in the stress-rate sensitivity of flexural strength in lightweight mortars. For the same impact velocity, the stress-rates experienced by a specimen was strongly influenced by its density. While the stress-rate sensitivity of flexural strength dropped with a decrease in the mix density, that of the fracture toughness was consistently higher for the lighter mixes.

1. Introduction

Perlite is an amorphous form of rhyolitic or dacitic magma that contains 2–5% water [1]. It transforms into a lightweight cellular material when heated to between 900 and 1000 °C. Its use in structural elements has been promoted in dynamically loaded members, where in the resulting reduction in the reactive mass is expected to limit the effect of earthquakes [2]. In most applications, it has been used as a replacement to Portland cement as a lightweight microfiller or to replace a portion of the sand. While its pozzolanic activity is acknowledged [3], its role in lightweight mortars is largely that of an inert aggregate [4].

Low density cement based composites may be divided into two categories: lightweight aggregate cementitious composites and foamed cement based composites. The former may further be classified into structural lightweight concrete and non-structural mortars (used mainly as insulation). Of these, foamed cement composites and non-structural mortars have crash cushioning abilities due to the manner in which they dissipate energy. An ideal shock absorbing material must possess high deformability, where the crushing strength is only important as a lower limit to the thickness of the barrier. Fig. 1 describes the typical load-deformation response of cellular solids [5], where the crushing strength is relatively low, but the composite is vastly deformable. The crushing strength is related to the buckling strength of the cell wall [6] where as overall deformability is related to the fracture toughness of the material in the cell wall. The plateau region in Fig. 1 describes the energy absorbing capacity in solids with significant cellular microstructure.

In designing cement based impact attenuators, lightweight, cellular inclusions such as expanded polystyrene, vermiculite and air bubbles have been used with varying degrees of success [7]. Recently, Le et al. [8] described damage due to high strain rates in high strength lightweight concrete. While lightweight aggregate concrete made with expanded perlite and vermiculite have been examined for shock absorption as far back as the 1960s [9], the quantification of material properties under dynamic loading has been limited with no information on their stress rate sensitivity and related dynamic fracture parameters. Further, much advancement has taken place in the succeeding decades through the introduction of short fibres for reinforcement. Both in conventional concrete and in structural lightweight concrete, such discrete fibre reinforcement is known to impart resistance under impact loading [10]. Where as steel fibres are most common in structural concrete, fibres such as those of glass, polypropylene and cellulose are known to perform better in controlled low strength materials, due to the compatibility in their strength and moduli [11].

This report is a part of a program to develop controlled low strength shock absorbing cement based composites for applications including rendering mortars, tunnel liners and similar protective construction through a suitable combination of modern

* Corresponding author. Tel.: +1 780 492 9661; fax: +1 780 492 0249.
E-mail address: vivek@ualberta.ca (V. Bindiganavile).

0958-9465/$ - see front matter © 2012 Elsevier Ltd. All rights reserved.
http://dx.doi.org/10.1016/j.cemconcomp.2012.10.004

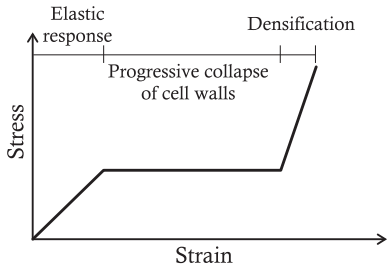

Fig. 1. Load-deformation response for an ideal energy absorbing material.

lightweight materials. The authors investigated controlled low strength lightweight mortars containing expanded aggregate fillers and polymeric microfibres. Specifically, the stress rate sensitivity of a range of lightweight mortars is examined through flexural testing of notched beams and the mechanical properties are related to the density of Portland cement paste.

2. Experimental details

2.1. Materials and mixes

Plain, unreinforced mixes were cast at four densities to examine a range of lightweight mortars between 1000 kg/m^3 and 2000 kg/m^3. The heaviest was effectively a cement paste that served as the reference, containing only Portland cement and a water-to-cement ratio of 0.4. Type GU Portland cement [12] as obtained from local suppliers was used in each mix. The remaining three lower densities were cast with increasing amounts of expanded perlite. The expanded perlite was sourced from a volcanic glass heated to 870 °C, resulting in a light weight material possessing a high specific surface area with properties as shown in Table 1. It had a bulk density of 64 kg/m^3 with a maximum particle size of 1.68 mm. As seen from Fig. 2a, the microstructure is characterised by open pores (small channels that form a thick network) and closed pores (isolated cells and holes). The simultaneous presence of these morphological features gives the mineral an extremely high transpiring power, due to the open pores, and at the same time, some crushing resistance in comparison with other lightweight fillers such as expanded polystyrene, due to the closed pores [13]. The former has led to its use in thermal insulation, while the latter has been utilised in structural lightweight concrete. In the present study, the addition of expanded perlite lightweight aggregate (EP) was defined by a volumetric ratio of EP with respect to Portland cement (PC), so that together with the reference mix, four mixes with volumetric ratios of 0, 0.8, 4, and 8 were produced. In order to be consistent with the water-to-cement ratio, a mini-slump cone was utilised to conduct a slump test (Fig. 3). The mixes were prepared to achieve a slump spread between 130 and 190 mm. Since the expanded perlite beads absorb a significant amount of the water added to the mix, an increase in the perlite content was compensated by a corresponding increase in the mix water. Accordingly, the water-to-cement ratio was 0.4 for the reference mix, and also for those containing volume ratio of EP-to-PC equal to 0.8 and 4. For the lightest mix with a volume ratio of EP-to-PC of 8, the water-to-cement ratio was raised to 0.8.

Table 1
Properties of expanded perlite used in this study.

Property	Value
Colour	White
Specific gravity	2.34
Bulk density (kg/m^3)	64
SiO_2 (%)	70–75
Al_2O_3 (%)	12–18
K_2O (%)	4–5
Na_2O (%)	3–4
CaO (%)	0.5–2
Fe_2O_3 (%)	0.5–1.5
MgO (%)	<0.5

Polymeric microfibres were chosen as discrete reinforcement due to their low modulus and high aspect ratio. The mixes in this investigation contained no coarse aggregate and as is well known, lightweight cementitious composites tend to be more brittle [14,15]. Therefore, an additional three mixes were reinforced with polypropylene microfibres that were 20 mm long with a maximum Denier count of 3 (in g/9000 m) and an elastic modulus of 3450 MPa (Fig. 2b). In order to retain adequate workability, a relatively low fibre volume fraction of 0.1% was considered. As there was no significant change in density for EP/PC equal to 0.8, only the reference cement paste and the two lightest mixes were reinforced with fibres. In spite of the low fibre content, workability continued to be a concern for the fibre reinforced mixes that also had expanded perlite. Hence, a combination of water reducing and/or air entraining admixtures were added to these mixes. In all cases, the mixes were designed for similar workability as expressed by the mini-slump cone test. Table 2 lists the mix designation and proportions for all seven mixes. Cylinders were cast to have 100 mm diameter and 200 mm height, while prisms were cast at 100 mm width × 100 mm height × 400 mm length to serve as beam specimens in flexure. The specimens were demolded after 24 h and placed in a curing chamber with controlled temperature (25 ± 2 °C) and humidity (100 ± 5% RH). The prisms were sawn to have notches 2 mm wide and 10 mm deep, to enable a study of crack growth. In each instance, at least six cylinders and beams were tested to produce the average data point for further analysis.

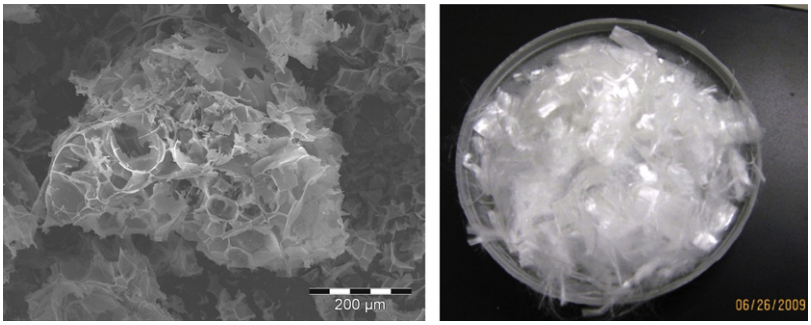

(a) SEM Image of Expanded Perlite (b) Polymeric Microfibre

Fig. 2. Lightweight aggregate and fibre reinforcement.

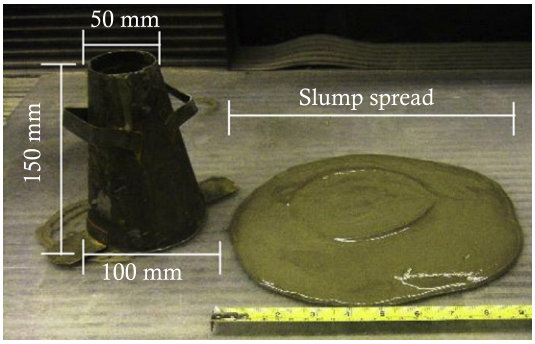

Fig. 3. Mini-slump cone test to measure the slump flow.

2.2. Test setup

2.2.1. Compression

The cylinders were tested in compression as per ASTM C469 [16] to obtain the constitutive stress–strain response until failure. Each cylinder was placed inside a collar that accommodated three linear variable displacement transducers (LVDTs) placed at 120° to each other as shown in Fig. 4a. The gauge length was kept equal to the diameter of the cylinder. In order to ensure a smooth and level surface in contact with the loading platens, the cylinders were end ground and further, during the test a piece of beaverboard was placed between the sample and each loading platen so as to smoothen any remaining unevenness in the sample. The compression test was performed in stroke control at a rate of 0.5 mm/min.

2.2.2. Flexure

2.2.2.1. Quasi-static test. The quasi-static flexural tests were done as per ASTM C1609 [17] to generate load and midspan deflection histories. These were used to determine the crack growth resistance via R-curves that in turn yielded the fracture toughness of the material. In order to create a prescribed crack path, each beam was sawn to produce a notch at midspan that was 10% of the overall depth. Fig. 4b shows schematically the size and location of the notch for each sample. The beams were subjected to four point bending with a span equal to three times the depth, i.e. 300 mm. In order to measure the mid-span deflection, LVDTs were mounted onto a yoke as described in the Japanese standard, JSCE-G 552 [18]. This yoke eliminates the need to account for load-point crushing, and any support settlement by measuring the true mid span deflection directly. The load was applied under stroke control with the loading head set to displace at 0.05 mm/min. The specimens were loaded until the onset of one of three conditions namely, complete failure, gradual load drop to zero, or upon reaching the full range of the LVDTs. In the case of the fibre reinforced specimens, the post peak response was considered up to a midspan deflection equal to 150th of the clear span.

2.2.2.2. Impact test. In the absence of a standard test method to evaluate the dynamic response of cement based materials, the mortar mixes were examined in flexure under impact from a drop-weight machine. The beams were loaded in three-point loading, with a span of 300 mm. Shown in Fig. 5, this system includes a 62 kg hammer which may be raised to a maximum height of 2.5 m. In this study, two rates of loading were generated as the specimens were subjected to a height of 250 mm and 500 mm, corresponding

Table 2
Mix design (mass expressed per 1 m^3).

Mix	Cement (kg)	Perlite (kg)	Water (kg)	Fibre (kg)	Water reducer (mL/kg of cement)	Air-entrainer (mL/kg of cement)	Hardened density (at test) kg/m^3
EP_0_0	1476	–	590	–	–	–	1970
EP_0.8_0.0	1290	21	572	–	0.26	–	1800
EP_4_0.0	1024	89	423	–	3.19	–	1440
EP_8_0.0	596	101	471	–	2.27	0.25	1030
EP_0_0.1	1472	–	589	0.879	–	–	1980
EP_4_0.1	1015	85	406	0.867	5.13	–	1460
EP_8_0.1	574	97	459	0.844	0.21	2.50	960

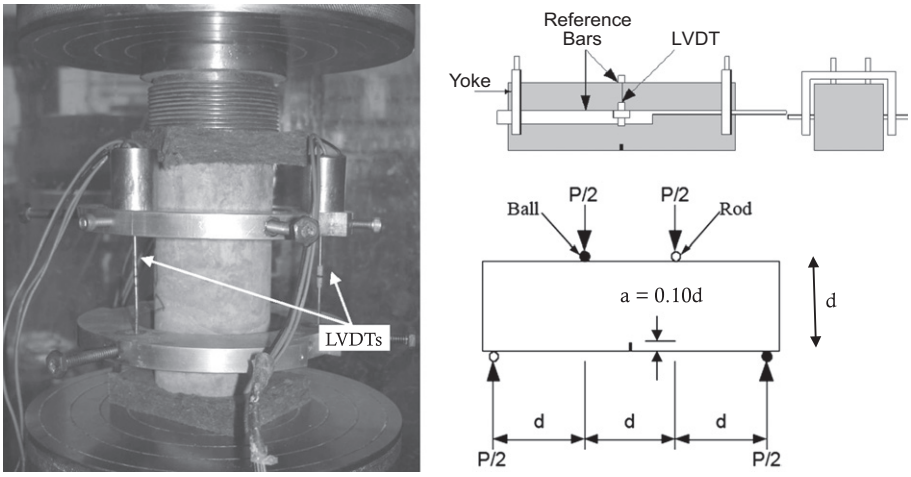

(a) Compression Test Setup (b) Flexural Test Setup

Fig. 4. Setups for the quasi-static tests.

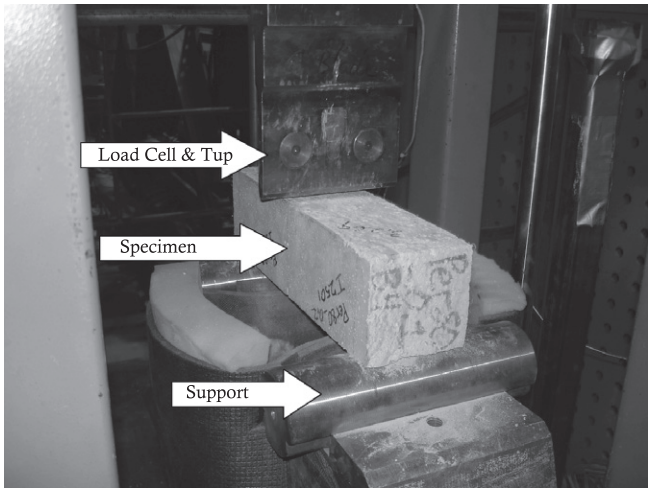

Fig. 5. Instrumented drop-weight impact tester.

to an impact velocity of 2.20 m/s and 3.10 m/s, respectively. The hammer tup was fitted with eight strain gauges that were arranged in two groups of four, to form a full Wheatstone bridge and serve as the load cell. The acceleration history was captured using a piezoelectric accelerometer that was attached to the bottom of the specimen at midspan. The acceleration and loading histories were both captured at 100 kHz through a data acquisition system triggered simultaneously. The data from the accelerometer was integrated twice with respect to time to yield the deflection history at midspan of the beam. Since a suddenly applied load creates an inertial response from the specimen, it is required that this inertia be accounted for to derive the flexural stresses on the beam as experienced by the material [19]. For a beam subjected to three-point bending under impact, the generalised inertial load on the specimen during the impact $P_i(t)$ is represented by [20]:

$$P_i(t) = \rho A a_o(t)\left[\frac{l}{3} + \frac{8(ov)^3}{3l^2}\right] \quad (1)$$

where, $a_o(t)$ is the acceleration at midspan of the beam at time, t; ρ the mass density for the beam material; A the cross-sectional area of the beam; l the clear span of the beam; ov is the length of overhanging portion of the beam.

Also, the velocity and displacement histories, $v_o(t)$, and, $d_o(t)$, at the load-point were obtained by integrating the acceleration history with respect to time:

$$v_0(t) = \int a_o(t)dt \quad (2)$$

$$d_0(t) = \int v_o(t)dt \quad (3)$$

3. Results and discussion

3.1. Compressive response

Fig. 6a shows the compressive stress–strain response for the plain mortar specimens, and it is seen that a moderate substitution of Portland cement with expanded perlite (EP/PC = 0.8) leads to a marginal increase in the compressive strength. The energy absorbed during compression is shown in Fig. 6b and was seen to decrease with an increase in the EP/PC ratio. The absorbed energy per unit volume (AE) was defined as the area within the stress–strain response up to a compressive strain of 1% and it is a measure of the energy dissipated by the mortar. In order to illustrate the effect of mix density on the mechanical performance, the mixes were normalised with respect to the Portland cement paste, to result in a relative density parameter, ρ_m/ρ_p. Accordingly, the variation in the compressive strength and the elastic modulus is shown in Fig. 7 for the plain mortars. Note that the compressive strength and elastic modulus scale as the cube of the relative density. According to Gibson and Ashby [6], the compressive strength of brittle cellular solids with an open cell structure varies as the 3/2 power with the relative density. Likewise, the same authors also indicate that the elastic modulus of open cell foams bears a quadratic dependence with relative density. Given the higher value of the exponent in the response in Fig. 7 one may conclude that cementitious mortars containing expanded perlite behave very different from cellular solids. As expected, there was no difference in the compressive response due to the addition of 0.1% volume fraction of fibres.

3.2. Flexural response

The flexural response of plain mortar beams is shown in Fig. 8 under quasi-static loading and Fig. 9 under impact loading. The failure was catastrophic immediately after reaching peak load and only the stable part of the response during the pre-peak phase is shown. Note that the quasi-static tests were performed under four-point bending whereas, under impact the notched beams were subjected to three-point bending. The flexural response of fibre reinforced mortars is shown under quasi-static loading in Fig. 10a and for impact loading in Fig. 10b–d. The fibre content was 0.1% by fraction of volume and due to the catastrophic failure under impact, the load–deflection response is shown up to peak load under dynamic conditions. The flexural response was analysed to evaluate the stress intensity factors as a function of the propagating crack from which the Mode-I fracture toughness, K_{IC}, was obtained for each mix for a specific loading condition. The procedure to derive the fracture toughness is described in detail in the Appendix.

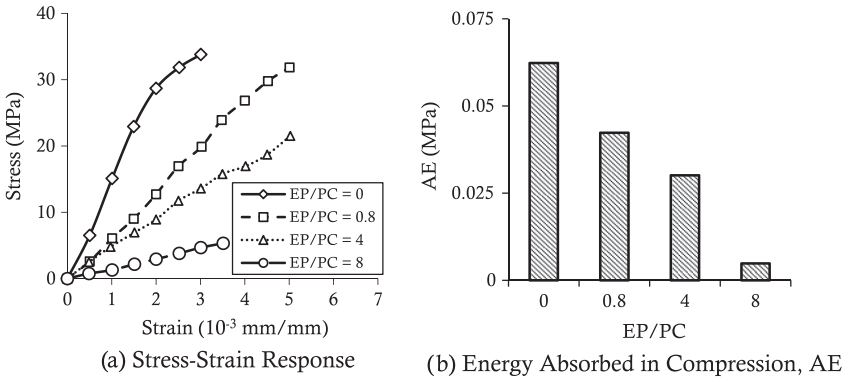

Fig. 6. Compressive response of plain lightweight mortars up to peak load.

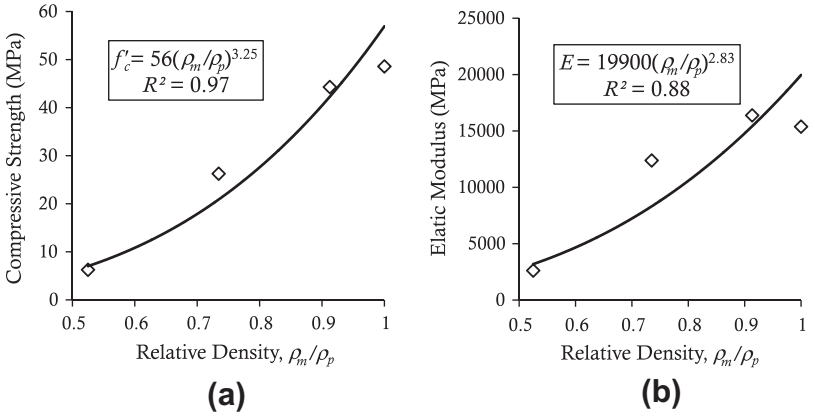

Fig. 7. Effect of relative density on: (a) compressive strength and (b) elastic modulus of plain mortars with varying amounts of expanded perlite; (note: ρ_m = density of any mix, ρ_p = density of Portland cement paste).

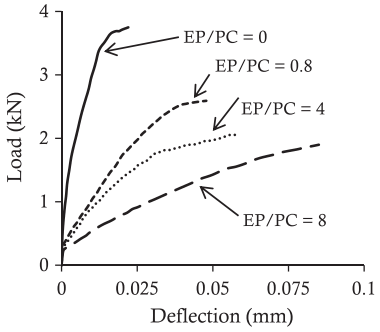

Fig. 8. Quasi-static response up to peak load for plain lightweight mortar beams containing varying amounts of expanded perlite.

The response of plain mortars under flexure is normalised with respect to their relative density in Fig. 11. Clearly, there exists an effect of density as well as an effect of loading rate. While the flexural strength under quasi-static loading scaled linearly with the relative density, under impact loading, the flexural strength depicted a quadratic relation under a 250 mm drop while it bore a cubic relation to relative density for a 500 mm drop. Similarly, the fracture toughness was affected by both density and loading rate so that, a linear relationship with relative density under quasi-static loading transformed into a power law for impact loading. As with plain mortars, the response of fibre reinforced mortars was normalised with respect to the density of the fibre reinforced Portland cement paste and is shown in Fig. 12 for all three cases of

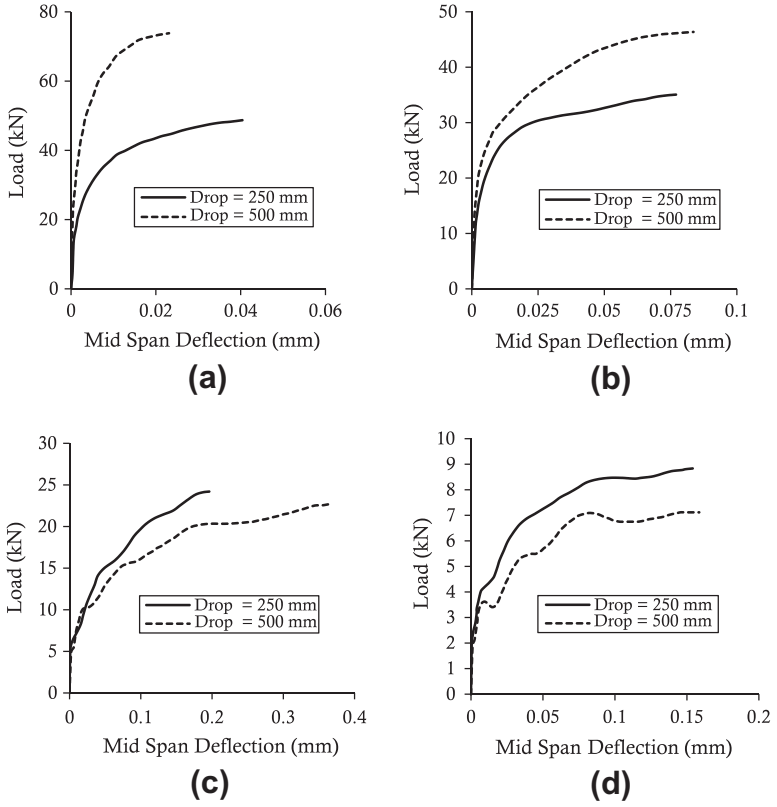

Fig. 9. Flexural response of plain lightweight mortars under impact loading up to peak for (a) EP/PC = 0; (b) EP/PC = 0.8; (c) EP/PC = 4; and (d) EP/PC = 8.

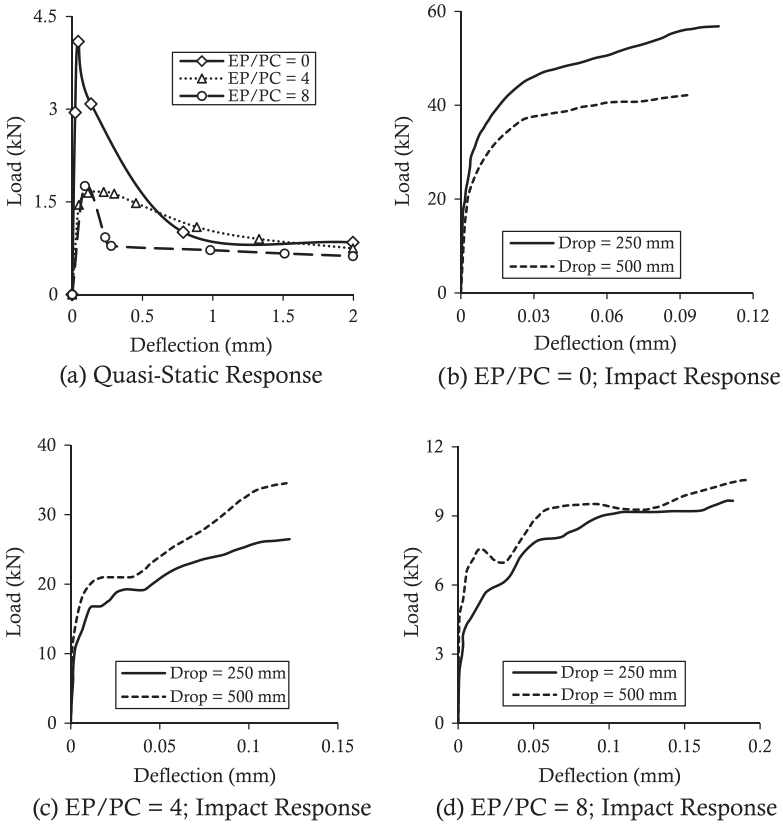

Fig. 10. Flexural response of lightweight mortars reinforced with 0.1% fibres, under (a) quasi-static loading and, impact loading up to Peak for (b) EP/PC = 0; (c) EP/PC = 4; and (d) EP/PC = 8.

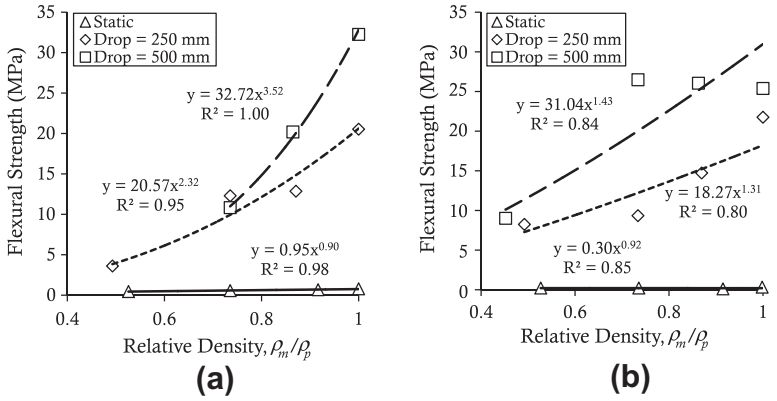

Fig. 11. Effect of relative density on the (a) flexural strength and (b) fracture toughness of plain mortars under static and impact loading (note: ρ_m = density of any mix, ρ_p = density of Portland cement paste).

loading. While both plain and fibre reinforced mortars exhibited similar linear scaling with relative density at quasi-static rates, the fibre reinforced mortars were more sensitive to relative density for higher rates of loading. As seen in Fig. 12b and c, the fracture toughness of fibre reinforced mortars was closer to a quadratic relation compared to the still almost linear scaling in the case of plain mortars even under impact loading.

Bindiganavile and Banthia [21] showed that the impact response of concrete as determined from drop-weight tests depends upon the hammer mass and the impact velocity. While some researchers have compared the effect of impact velocity on lightweight mortars [5], it was noted here that defining the dynamic behaviour with respect to the impact velocity was not appropriate: Although subjected to identical impact velocities from the same drop height, the stress rate experienced by a specimen was seen to depend on its density. As seen from Fig. 13, the stress rate experienced by the lightest mortar was about 1/20th of that experienced by the Portland cement paste, although the paste weighed only twice as much. Since the compressive strength for each density was different, a direct comparison of test results was not feasible. Hence, a dynamic amplification factor (DAF) was defined as the ratio between the mechanical parameter at dynamic stress rates to the corresponding quasi-static value. The stress rate sensitivity of a mechanical property of concrete may be described by means of a bilinear response according to the formulation given by Nadeau et al. [22]. Eq. (4) expresses this response for each leg

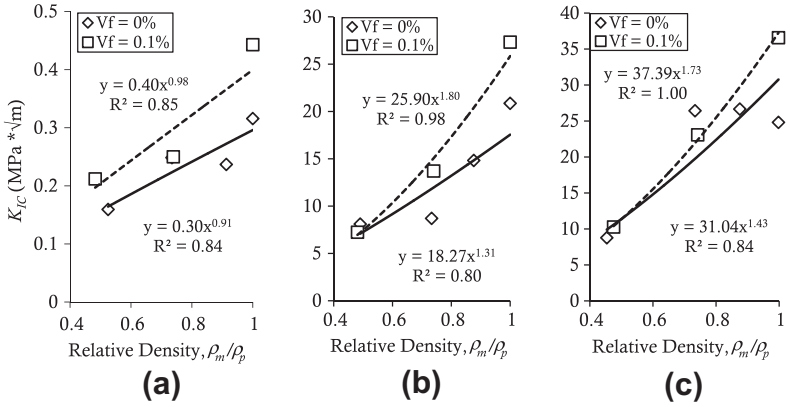

Fig. 12. Effect of fibres on the density scaling of fracture toughness for mortars under (a) quasi-static loading, and under impact from (b) 250 mm and (c) 500 mm (note: ρ_m = density of any mix, ρ_p = density of Portland cement paste).

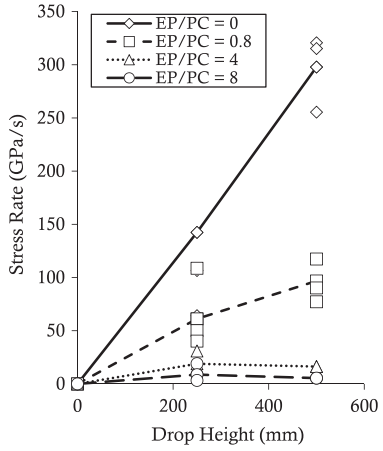

Fig. 13. Stress rate as a function of drop height.

of the bilinear plot, where $\dot{\sigma}_{dyn}$ and $\dot{\sigma}_{st}$ refer to the dynamic and reference quasi-static stress rates, respectively.

$$\log(DAF) = \frac{1}{N+1}\log\frac{\dot{\sigma}_{dyn}}{\dot{\sigma}_{st}} + Constant \quad (4)$$

Eq. (4) was derived based on crack kinetics in a brittle material, seen experimentally to fit $da/dt = AK_I^N$ where the crack velocity, da/dt, was related exponentially to the stress intensity factor, K_I, with an exponent equal to N. It is understood that the smaller the value of N, the higher the stress rate sensitivity. The stress rate sensitivity of all plain mortars is shown in Fig. 14a, for flexural strength and Fig. 14b for fracture toughness. Note that the value of N shown corresponds to the higher stress rates conducted under impact loading. Whereas the flexural strength became less sensitive to stress rate for an increase in the EP/PC ratio, the reverse was true for fracture toughness, so that mortars of lower density were also more rate sensitive. As seen in Fig. 15, the addition of fibres made the flexural strength of the densest mix less stress rate sensitive. This is in keeping with previous work on plain and fibre reinforced concrete [23], where in the latter is uniformly known to be less sensitive. However, for lower densities, the flexural strength of the mortar was always more sensitive to stress rate upon the addition of fibres. On the other hand, the stress rate sensitivity of fracture toughness in the Portland cement paste – the densest mix in the series – was higher upon adding fibres, but in the lighter mortars containing expanded perlite, the addition of fibres reduced the stress rate sensitivity of K_{IC}. This is shown in Fig. 16. In summary, the higher rate sensitivity of fracture toughness in lighter mortars may be exploited in the construction of protective systems where by the lightweight cementitious composite forms the sacrificial component that absorbs the initial shock.

4. Concluding remarks

The following conclusions are drawn based on the results reported in this paper:

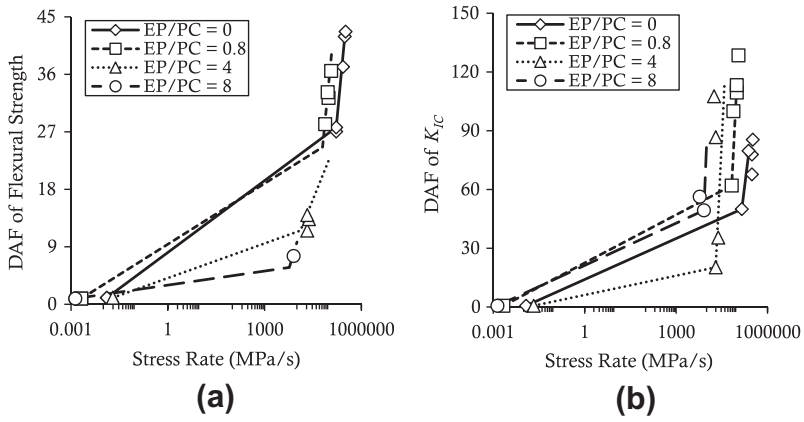

Fig. 14. Stress-rate sensitivity of (a) flexural strength; and (b) fracture toughness of plain mortar containing various amount of expanded perlite.

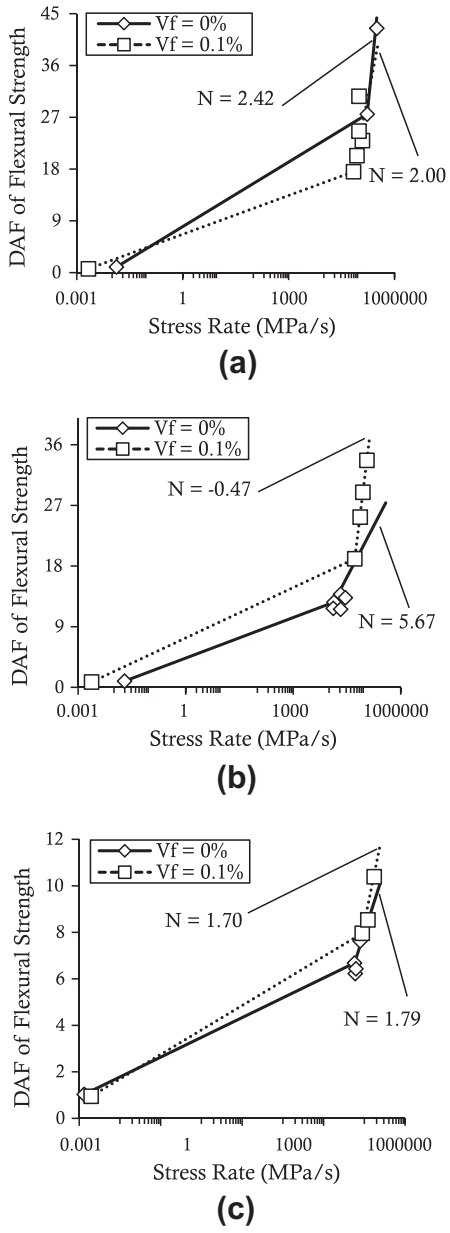

Fig. 15. Stress rate sensitivity of flexural strength for plain and fibre reinforced mortar containing (a) EP/PC = 0%; (b) EP/PC = 4; and (c) EP/PC = 8.

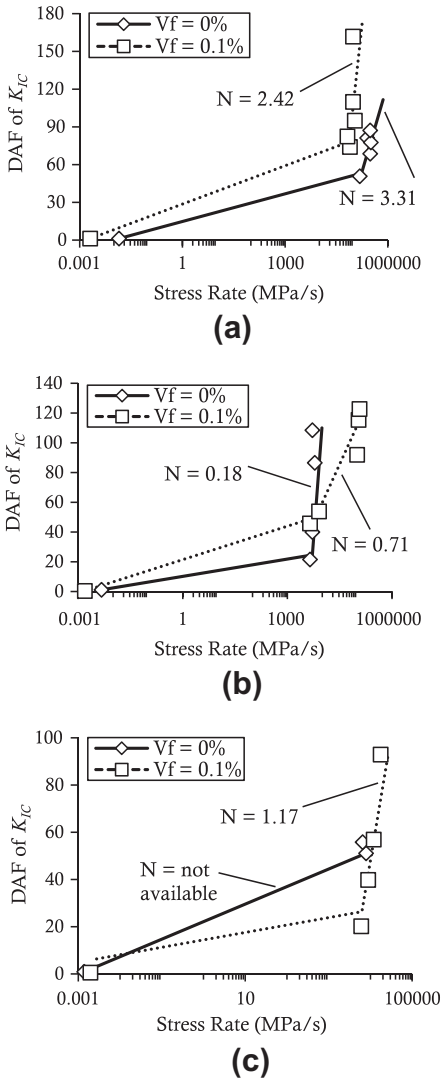

Fig. 16. Stress rate sensitivity of Mode I fracture toughness for plain and fibre reinforced mortar containing (a) EP/PC = 0%; (b) EP/PC = 4; and (c) EP/PC = 8.

- In plain mortars under compression, the addition of expanded perlite leads to a density scale effect for strength and elastic modulus under compression. Both strength and elastic modulus scale as the cube of the relative density, defined as the ratio of the density of the mortar to that of Portland cement paste.
- In plain mortars subjected to bending under quasi-static loads, both strength and fracture toughness scale linearly with the relative density of the mix. However, under impact loading, the flexural strength and Mode-I fracture toughness are more sensitive to the density of the mixture.
- The fracture toughness of fibre reinforced cementitious mortars is more sensitive to the relative density than that of plain unreinforced mixes. The difference in sensitivity between plain and fibre reinforced mortars is more pronounced during their impact response.
- In lightweight cement based mortars, the stress rate experienced under identical velocity of impact strongly depends upon the density of the composite. For the range of mixes examined, a two fold increase in weight resulted in a 20-fold increase in the stress rate experienced.
- Reinforcing lightweight mortars that contain expanded perlite with polymer microfibres affects the stress rate sensitivity of their flexural strength and Mode I fracture toughness. While the flexural strength becomes more rate sensitive, the latter was seen to be less sensitive to stress rate in the presence of fibres.

Acknowledgement

The financial support from the Natural Sciences and Engineering Research Council (NSERC), Canada is gratefully acknowledged.

Appendix A. Derivation of fracture toughness from R-curves

The R-curve is a measure of the material's resistance to crack growth. In this paper the R-curve is presented as the stress intensity factor (K_I) plotted against the effective crack length divided by the depth of the section (a_{eff}/d). The method used to determine the R-Curve for a specimen was adopted from Kraft et al. [24] by varying

the notch length of each specimen to find the corresponding stress intensity factor. Instead of multiple specimens with varying initial notch lengths, the progressively growing crack of one sample is used. The stress intensity factor is dependent on the nominal stress on the section and the crack length. The nominal stress was defined as per Eq. (A1), and solved for four point bending where, P was the overall load applied to the system, b, d and S were respectively the width, the depth and the span of the beam.

$$\sigma = \frac{PS}{bd^2} \tag{A1}$$

While the derivation for stress intensity factors is based on LEFM, the assumption that the fracture process zone ahead of the crack tip is small enough to have negligible plasticising effect is not valid for cement based materials. An effective crack is used to model the existing crack as a straight traction-free crack of a length equal to the length of the true crack plus the length of the fracture process zone. This leaves only an elastic material outside of the crack and therefore allows the use of LEFM. The method to find the effective crack length was adopted from Banthia and Sheng [25] who used a compliance calibration.

In order to determine the length of an effective crack, a_{eff}, one must first relate the crack length and the crack mouth opening displacement, CMOD, by an equation from LEFM. Such equations may be found in stress analysis handbooks and Eq. (A2) is taken from Tada et al. [26] for a beam of finite width, with a single edge notch undergoing pure bending. In Eq. (A2) 'a' is the crack length and 'b' is the characteristic length of the specimen, which in this case is also the height of the beam. The multiplying function $V(a/b)$ adjusts the original expression which was derived for an infinite plate containing a centre crack, to be applicable to the given case. For a single edge notch in a beam subjected to pure bending, $V(a/b)$ is taken from Tada et al. [26] as expressed in Eq. (A3). The correction factor so expressed was found to be accurate to within 1% error for any a/b.

$$\text{CMOD} = \frac{4\sigma a}{E} V(a/b) \tag{A2}$$

$$V(a/b) = 0.8 - 1.7(a/b) + 2.4(a/b)^2 + \frac{0.66}{(1-a/b)^2} \tag{A3}$$

Since the crack mouth opening displacement was not measured directly during the test, it was interpreted from the load vs. deflection diagram as suggested by Armelin and Banthia [27]. As shown there in, during the course of a bending test, the CMOD bears a linear relationship with the midspan deflection δ and is about 33% higher in value, Eq. (A4). This result was confirmed in the case of impact loading by Chan [28]. By assuming that the material ahead of the effective crack is linear elastic, Eq. (A2) may be rearranged to determine its elastic modulus for each point along a load–CMOD graph as shown by Eq. (A5). Further, the elastic modulus is a constant and therefore it must be true that by taking a point at the initial portion of the load–CMOD curve where the crack has not progressed further than the initial notch length, a_o, the elastic modulus so derived may be equated to that at a point further along the load–CMOD curve corresponding to a new crack length, a_{eff}, which is now the length of an effective crack corresponding to that point on the load–CMOD curve. In this manner, one evaluates the corresponding effective crack length, a_{eff}. Note that the load–CMOD response for the dynamic case was obtained after accounting for specimen inertia.

$$\frac{d\text{CMOD}}{d\delta} = \frac{4}{3} \tag{A4}$$

$$E = 6\left(\frac{P}{\text{CMOD}}\right)\frac{a_o S}{bd^2} V(a_0/b) = 6\left(\frac{P}{\text{CMOD}}\right)\frac{a_{eff} S}{bd^2} V(a_{eff}/b) \tag{A5}$$

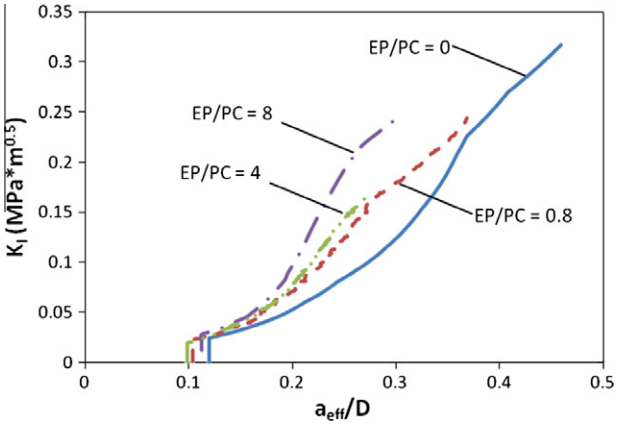

Fig. A1. Representative R-curves for plain mortar beams having varying amounts of expanded perlite.

Thus, at each load level, the corresponding stress intensity factor may be determined by Eq. (A6) to produce R-curves. As an illustration, representative quasi-static R-curves for plain mortars examined in this study are shown in Fig. A1. Again, as Eq. (A6) is derived from the condition of an infinite plate with a centre crack, a geometric correction factor, $F_1(a/b)$, is applied to adjust the original result for practical cases. This factor for an edge notch with finite width undergoing pure bending is presented in Eq. (A7) and is known to have an accuracy of better than 0.5% for any value of a/b less than 1. The peak value in the $K_I - a_{eff}$ graph is the critical stress intensity factor (K_{IC}), or the fracture toughness. The corresponding critical crack length (a_{effc}) was also noted.

$$K_{Ieff} = \sigma_n \sqrt{a_{eff}} F_1(a_{eff}/b) \tag{A6}$$

$$F_1(a/b) = \sqrt{\frac{2b}{a}} tan\left(\frac{a}{2b}\right) \frac{0.923 + 0.199(1 - sin\left[\frac{a}{2b}\right])^4}{cos\left(\frac{a}{2b}\right)} \tag{A7}$$

References

[1] Mladenovic A, Suput JS, Ducman V, Skapin AS. Alkali–silica reactivity of some frequently used lightweight aggregates. Cem Concr Res 2004;34:1809–16.
[2] Topçu IB, Işikdağ B. Effect of expanded perlite aggregate on the properties of lightweight concrete. J Mater Proc Technol 2008;204(1–3):34–8.
[3] Yu L-H, Ou H, Lee L-L. Investigation of pozzolanic effect of perlite powder in concrete. Cem Concr Res 2003;33:73–6.
[4] Lanzón Torres M, García-Ruiz PA. Lightweight pozzolanic materials used in mortars: evaluation of their influence on density, mechanical strength and water absorption. Cem Concr Compos 2009;31:114–9.
[5] Bischoff PH, Yamura K, Perry SH. Polystyrene aggregate concrete subjected to hard impact. In: Proc. Inst. Civ. Engrs, Part 2, vol. 89, June; 1990. p. 225–39.
[6] Gibson LJ, Ashby MF. Cellular solids: structure and properties. 2nd ed. Cambridge University Press; 1997.
[7] Bakos JD. Scale model study of low density concrete impact attenuators. Accession number PB2843779, Ohio DOT; 1978. p. 191.
[8] Le JL, Koh CG, Wee TH. Damage modeling of high strength lightweight concrete under impact. Mag Concr Res 2006;58(6):343–55.
[9] Smith E, Thompson JN. A study of vermiculite concrete as a shock isolating material, Accession no: AD0431606, Defence Technical Information Center, Fort Belvoir, VA; 1963. p. 247.
[10] Zhang ML, Li L, Paramasivam P. Flexural toughness and impact resistance of steel fibre reinforced lightweight concrete. Mag Concr Res 2004;56(5):251–62.
[11] Lin W, Wang H. Glass fiber reinforced lightweight concrete modified with polymer latex. In: Proceedings: international symposium on fibre reinforced cement and concrete, RILEM, Sheffield UK; 1992. p. 921–25.
[12] CAN/CSA A 23.1. Concrete materials and methods of concrete construction/ methods of test and standard practices for concrete. Canadian Standards Association; 2004.
[13] Perlite Italiana. What is Perlite? 2009. <http://www.perlite.it/en/CosaPerlite.asp>.
[14] Zhang M-H, Grørv OE. Microstructure of the interfacial zone between lightweight aggregate and cement paste. Cem Concr Res 1990;20:610–8.

[15] Yang K-H, Ashour AF. Aggregate interlock in lightweight concrete continuous deep beams. Engineering Structures 2011;33:136–45.
[16] ASTM C469.. Standard test method for static modulus of elasticity and poisson's ratio of concrete in compression. West Conshohocken (PA): ASTM International; 2002.
[17] ASTM C1609–05. Standard test method for flexural performance of fiber-reinforced concrete – using beam with third-point loading. West Conshohocken (PA): ASTM International; 2005. p. 8.
[18] JSCE-G 552. Test method for bending strength and bending toughness of steel fiber reinforced concrete. Japan Society of Civil Engineering; 1999.
[19] Chen EP, Sih GC. Transient response of cracks to impact loads. Mechanics of fracture, 4: Elastodynamic crack problems; 1977. p. 1–58.
[20] Banthia NP, Mindess S, Bentur A, Pigeon M. Impact testing of concrete using a drop-weight impact machine. Exp Mech 1989;29(12):63–9.
[21] Bindiganavile V, Banthia N. Machine effects in the drop-weight impact testing of plain concrete beams. In: Proceedings: 3rd international conference on concrete under severe conditions (CONSEC'01), vol. 1. BC (Canada): Vancouver; 2001. p. 589-96.
[22] Nadeau JS, Bennett R, Fuller Jr ER. An explanation for the rate-of-loading and the duration-of-load effects in wood in terms of fracture mechanics. J Mater Sci 1982;17:2831–40.
[23] Bindiganavile V, Banthia N. Generating crack growth resistance curves for fiber reinforced concrete. Exp Mech 2005;45(2):112–22.
[24] Kraft JM, Sullivan AM, Boyle RW. Effect of dimensions on fast fracture instability of notched sheets. In: Proceedings: crack propagation symposium, College of Aeronautics, Cranfield, UK, vol. 1; 1961. p. 8.
[25] Banthia N, Sheng J. Fracture toughness of micro-fiber reinforced cement composites. Cem Concr Compos 1996;18(4):251–69.
[26] Tada H, Paris PC, Irwin GR. The stress analysis of cracks handbook. 3rd ed. ASME; 1985. p. 58–60.
[27] Armelin HS, Banthia N. Predicting the flexural postcracking performance of steel fibre reinforced concrete from the pullout of single fibres. ACI Mater J 1997;94(1):18–31.
[28] Chan R. Static and dynamic fracture toughness of plain and fibre reinforced hydraulic lime mortars. MSc Thesis, University of Alberta, Edmonton, September; 2009. p. 170.